Synthesis, Physicochemical Characterization, and Biological Evaluation of 2-(1′-Hydroxyalkyl)-3-hydroxypyridin-4-ones: Novel Iron Chelators with Enhanced pFe^{3+} Values†

Zu D. Liu, Hicham H. Khodr, Ding Y. Liu, Shu L. Lu, and Robert C. Hider*

Department of Pharmacy, King's College London, 150 Stamford Street, London SE1 8AW, U.K.

Received May 17, 1999

The synthesis of a range of 2-(1′-hydroxyalkyl)-3-hydroxypyridin-4-ones as bidentate iron(III) chelators with potential for oral administration is described. The pK_a values of the ligands and the stability constants of their iron(III) complexes have been determined. Results indicate that the introduction of a 1′-hydroxyalkyl group at the 2-position leads to a significant improvement in the pFe^{3+} values. Such an effect was found to be greater with the hydroxyethyl substituent than with the hydroxymethyl substituent, particularly in the cases of 1-ethyl-2-(1′-hydroxyethyl)-3-hydroxypyridin-4-one ($pFe^{3+} = 21.4$) and 1,6-dimethyl-2-(1′-hydroxyethyl)-3-hydroxypyridin-4-one ($pFe^{3+} = 21.5$) where an enhancement on pFe^{3+} values in the region of two orders of magnitude is observed, as compared with Deferiprone (1,2-dimethyl-3-hydroxypyridin-4-one) ($pFe^{3+} = 19.4$). The ability of these novel 3-hydroxypyridin-4-ones to facilitate the iron excretion in bile was investigated using a [^{59}Fe]ferritin-loaded rat model. Chelators and prodrug chelators possessing high pFe^{3+} values show great promise in their ability to remove iron under *in vivo* conditions.

Introduction

The most frequent treatment of inherited hematological diseases such as β-thalassemia major is to maintain high levels of hemoglobin by regular blood transfusion. Repeated transfusion leads to elevated body iron levels due to the inability of humans to excrete iron *via* the kidney. Excess iron is mainly located within the liver and other highly perfused organs leading to tissue damage, organ failure, and eventually death.[1] Complications associated with elevated iron levels can be largely avoided by the use of iron-specific chelating agents and in particular desferrioxamine (DFO). Unfortunately, DFO lacks oral activity, and this has a dramatic influence on patient compliance.[2]

3-Hydroxypyridin-4-ones (HPOs) are currently one of the main candidates for the development of orally active iron chelators.[3] Indeed, the 1,2-dimethyl derivative CP20 (Deferiprone, L1) (**1**) (Table 1) is currently in clinical trials. Unfortunately, the dose required to keep a previously well-chelated patient in negative iron balance appears to be relatively high. Not surprisingly therefore, side effects have been observed in some patients receiving CP20.[4] One of the major reasons for the limited efficacy of CP20 in clinical use is that it undergoes extensive phase II metabolism in the liver. The 3-hydroxyl functionality, which is crucial for scavenging iron, is also a prime target for phase II conjugation. Urinary recovery studies conducted on CP20 in both rats and humans have shown that respectively >44% and >85% of the administered dose is recovered in the urine as the non-chelating 3-*O*-glucuronide conjugate.[5] This extensive biotransformation limits its ability to mobilize excess body iron in thalassemic patients.

The 1,2-diethyl analogue CP94 (**2**) (Table 2) has also been widely investigated.[6−9] This chelator was found to be much more efficient at iron removal than CP20 in several mammalian species, e.g. mice,[6] rat,[7] and primate,[8] whereas it was ineffective at mobilizing iron in guinea pig[7] and human[9] due to extensive 3-*O*-glucuronide conjugation. One of the presumed reasons for the greater efficacy of CP94 in the rat is its unusual phase I metabolic pathway which leads to the formation of the 2-(1′-hydroxyethyl) metabolite **3** (Scheme 1).[5] This metabolite does not undergo further phase II metabolism to form a glucuronide conjugate and hence retains the ability to chelate iron. However such an explanation may well be an oversimplification since other 1-hydroxyalky HPOs, namely **4** and **5** (Table 1), are also not extensively metabolised *via* phase II reactions[10] and yet their iron mobilization efficacies in rats are much less than that of CP94.[11] The same observation holds for their ester prodrugs such as **6** and **7** (Table 1). Thus it was decided to investigate the properties of the 2-(1′-hydroxyethyl) metabolite of CP94. In this work we describe the synthesis, physical−chemical properties, and *in vivo* iron mobilization efficacies of a range of novel 2-(1′-hydroxyalkyl) derivatives of 3-hydroxypyridin-4-ones.

Chemistry

A furfuryl alcohol-based method has been developed for the preparation of the key starting material, pyromeconic acid (**12**) (Scheme 2). Bromination of furfuryl alcohol (**8**) in buffered methanol leads to the formation

* Corresponding author: Robert C. Hider. Tel: 20 7848 4646. Fax: 20 7848 4195. E-mail: robert.hider@kcl.ac.uk.

† Abbreviations: pFe^{3+}, the negative logarithm of the concentration of the free iron(III) in solution, calculated for total [ligand] = 10^{-5} M, total [iron] = 10^{-6} M at pH 7.4; DFO, desferrioxamine; HPO, hydroxypyridinone; CP20, 1,2-dimethyl-3-hydroxypyridin-4-one; CP94, 1,2-diethyl-3-hydroxypyridin-4-one; $D_{7.4}$, distribution coefficient at pH 7.4; MOPS, 4-morpholinopropanesulfonic acid;

10.1021/jm991080o CCC: $18.00
Published on Web 10/28/1999

Table 1. Chemical Structure of Selected 3-Hydroxypyridin-4-ones

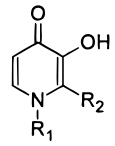

compd	R_1	R_2	MW	$D_{7.4}$	log *P*	efficacy (%)[a]
CP20 (**1**)	CH_3	CH_3	139	0.17	−0.77	9.5
CP94 (**2**)	CH_2CH_3	CH_2CH_3	167	1.78	0.25	55.8
3	CH_2CH_3	$CH(OH)CH_3$	183	0.26	−0.58	50.6
4	CH_2CH_2OH	CH_2CH_3	183	0.22	−0.66	12.9
5	$(CH_2)_3OH$	CH_3	183	0.13	−0.89	26.0
6	$CH_2CH_2OOC(CH_3)_3$	CH_2CH_3	267	14.5	1.16	19.1
7	$(CH_2)_3OOCC_6H_5$	CH_3	287	17.6	1.25	32.5

[a] Iron mobilization efficacy (%) of the chelators was measured on the [^{59}Fe]ferritin-loaded rat model.[11]

Scheme 1. Metabolism of CP94 via Phase I and Phase II Metabolic Pathways[a]

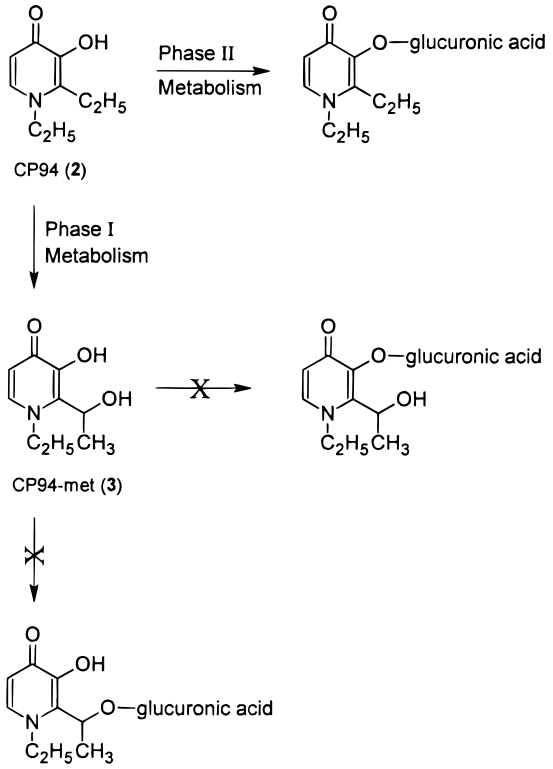

[a] The 2-1′-hydroxylated metabolite (**3**) is the major metabolite in rat, whereas the phase II glucuronidation is the major metabolism of CP94 in humans.

Scheme 2. Synthesis of Pyromeconic Acid (**12**) from Furfuryl Alcohol

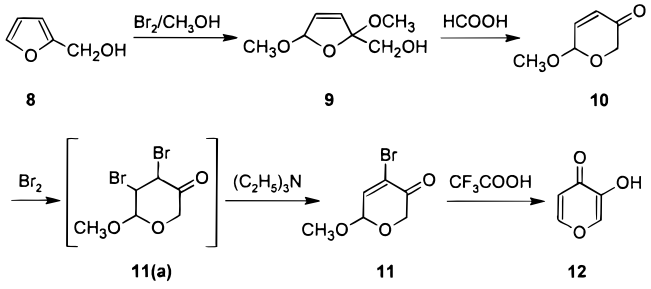

of a mixture of the *cis* and *trans* isomers of 2,5-dihydro-2,5-dimethoxy-2-furanylmethanol (**9**). Mild acid hydrolysis of **9** in formic acid brings about cleavage of the acetal bond and subsequent ring expansion to form 6-methoxy-2*H*-pyran-3(*6H*)-one (**10**), which is then smoothly converted to the 4-bromo-6-methoxy-2*H*-pyran-3(*6H*)-one (**11**) in a good yield (82%) by treatment with 1 equiv of bromine and 1 equiv of an organic base, e.g. triethylamine. The conversion of **10** to **11** may proceed *via* the labile 4,5-dibromo derivative **11a** which has not been isolated in this sequence. Pyromeconic acid (**12**) can then be prepared from the acid-induced rearrangement of **11** using concentrated trifluoroacetic acid (yield: 80%).

Scheme 3. Synthesis of Allomaltol (**15**)

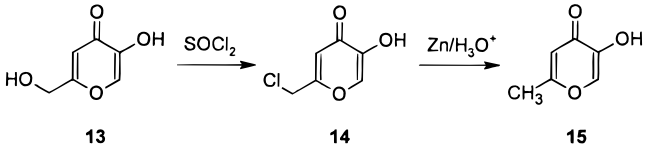

Scheme 4. Synthesis of 2-(1′-Hydroxyalkyl)-3-hydroxypyran-4-ones **16a**−**16e**

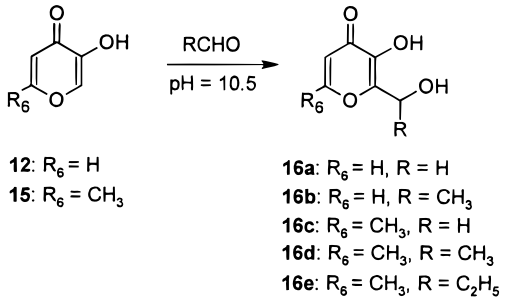

The synthesis of pyromeconic acid (**12**) by one-pot reaction starting from furfuryl alcohol (**8**) has also been attempted; however extensive decomposition was observed, resulting in poor yields (less than 20%) (unpublished data).

The synthesis of allomaltol (**15**) can be readily accomplished using commercially available kojic acid (**13**) in a two-step reaction (Scheme 3). The 2-position of both pyromeconic acid (**12**) and allomaltol (**15**) can be functionalised in an analogous fashion to the aldol condensation whereby the pyrone anion aldehyde, under alkaline aqueous conditions, furnishes, on acidic work-up, the 2-(1′-hydroxyalkyl)-3-hydroxypyran-4-one (**16**) in high yields (80−90%) (Scheme 4). The pH of the reaction solution was found to be critical, since highly alkaline conditions resulted in extensive aldehyde polymerization. The optimal pH for this reaction was found to be approximately 10.5.

Scheme 5. Synthesis of 2-(1′-Hydroxyalkyl)-3-hydroxypyridin-4-ones **19**

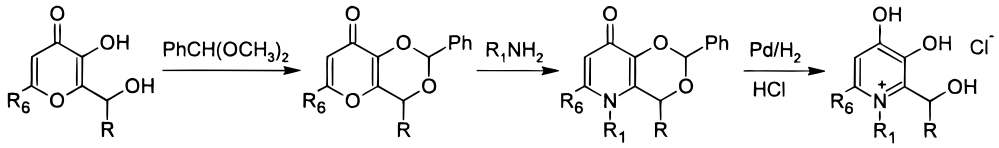

16 **17** **18** **19**

Scheme 6. Synthesis of the Benzoyl Ester Derivative **21**

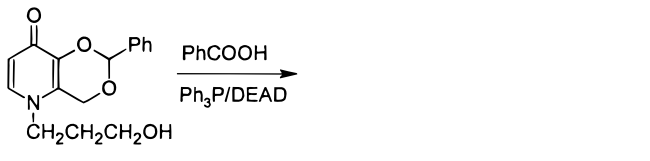

18d

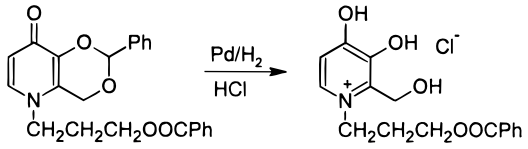

20 **21**

The general methodology adopted for the synthesis of 2-(1′-hydroxyalkyl)-3-hydroxypyridin-4-ones is summarised in Scheme 5. The protection of the 2-(1′-hydroxyl) function proved to be essential since without protection, marked decomposition was observed, which consequently resulted in low yields (<10%). In the current work, both the 3-hydroxyl and the 2-(1′-hydroxyl) groups were protected in one step by reacting corresponding pyran-4-ones **16** with benzaldehyde dimethyl acetal in *N*,*N*-dimethylformamide in the presence of a catalytic amount of toluene-*p*-sulphonic acid. The desired pyridinone products **19** were then prepared by the reaction of the protected pyranone **17** with a range of primary amines, followed by hydrogenation to remove the protecting group. Generally, 2-monosubstituted pyran-4-one derivatives can react with various primary amines under mild conditions, e.g. stirring at ambient temperature or refluxing in aqueous alcohol, resulting with the conversion to the corresponding pyridin-4-one analogous in good yields.[12,13] However, the analogous reaction between 2,6-disubstituted pyran-4-ones and amines is limited to primary amines of short chain length (such as methylamine or ethylamine) since longer chain lengths or branching results in yields of less than 5% (unpublished data). This may be attributed to the flanking 2- and 6-substituents providing a steric barrier to ring closure resulting in high yields of polymeric side products.

A benzoyl ester prodrug has been prepared by reacting the protected alcohol **18d** with benzoic acid in the presence of triphenylphosphine and diethyl azodicarboxylate (Scheme 6).[14] After hydrogenation, the final compound **21** was isolated as the hydrochloride salt.

Physicochemical Characterization

3-Hydroxypyridin-4-ones possess two pK_a values, one corresponding to the 4-hydroxyl function and the second corresponding to the 3-hydroxyl function. These bidentate ligands also form a number of complexes with iron(III) so that aqueous solutions equilibrate to give a mixture in which the speciation depends on the metal ion, ligand, and hydrogen ion concentration. In order to investigate the influence of the 2-(1'-hydroxyalkyl) substituent on ligand affinity, both the pK_a values of the ligands and the stability constants of their iron(III) complexes were evaluated using a combined automated spectrophotometric and potentiometric titration system.[12,13] Distribution coefficients of the chelators were measured using an automated continuous flow technique.[12,13]

Biological Experiments

In vivo iron mobilization efficacy of all ligands was evaluated in a non-iron-overloaded rat model originally developed by Pippard et al.[15] [^{59}Fe]Ferritin is used to label the liver iron pool, and this is followed by a challenge with a test chelator at a time when the iron released by lysosomal degradation of ferritin is maximally available.[11,15] Since the liver is the major iron storage organ under iron-overloaded conditions, this method comes close of being an ideal animal model to assess oral bioavailability and to compare the ability of chelators to remove iron from liver. In this model, DFO, Deferiprone, and diethylenetriaminepentaacetic acid (DTPA) all behave in a manner similar to that observed clinically.[11,15] Furthermore this method produces highly reproducible data of the type necessary for dose−response investigations and structure−activity studies.[15]

Results

Ligand pK_a Values. All ligands were investigated by simultaneous spectrophotometric and potentiometric titration. The optimized pK_a values obtained from nonlinear least-square regression analysis are shown in Table 4. The pK_{a1} values correspond to the deprotonation of the 4-hydroxy group and the pK_{a2} values to the dissociation of the 3-hydroxy group (Scheme 7). The pK_a values obtained from spectrophotometric titration are similar and comparable to those calculated from the potentiometric titration (Table 4). This indicates that it is valid to use the pK_a values obtained by simultaneous titration to support the experimental work. The introduction of a 1′-hydroxyalkyl function at the 2-position results in clear reduction in the pK_a values of both the 4-hydroxyl and 3-hydroxyl groups, as compared with simple alkyl-substituted HPOs such as CP20 and CP94 (Table 4). Such an effect was found to be greater with the hydroxyethyl substituent than with the hydroxymethyl substituent, particularly in the cases of ligands **3** (pK_{a2} = 8.76 ± 0.02) and **19e** (pK_{a2} = 8.71 ± 0.01), where a reduction in pK_a values of the 3-hydroxyl group in the region of one order of magnitude was observed, as compared with CP20 (pK_{a2} = 9.71 ± 0.06).

Table 2. Chemical Structure of Compounds **17**, **18**, and **20**

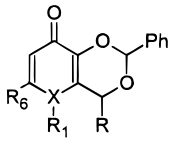

compd	X	R_1	R	R_6
17a	O		H	H
17b	O		CH_3	H
17c	O		H	CH_3
17d	O		CH_3	CH_3
17e	O		C_2H_5	CH_3
18a	N	CH_3	H	H
18b	N	C_2H_5	H	H
18c	N	C_2H_5	CH_3	H
18d	N	$CH_2CH_2CH_2OH$	H	H
18e	N	$CH_2CH_2CH_2OH$	CH_3	H
18f	N	CH_3	H	CH_3
18g	N	C_2H_5	H	CH_3
18h	N	CH_3	CH_3	CH_3
18i	N	CH_3	C_2H_5	CH_3
20	N	$CH_2CH_2CH_2OOCPh$	H	H

Stability Constants of Iron(III) Complexes. In a multicomponent solution the absorbance at a single wavelength is given by the sum of the absorbances of the individual species present. When full spectra are recorded the observation of a shift in λ_{max} at differing metal/ligand equilibrium conditions is the most direct evidence of a multicomponent system. Analysis of the resultant absorbance spectra obtained from a solution of metal/ligand at various pH values permits the calculation of the concentration of each species as a function of pH and hence the stability constant. In this current work, the stability constants of all bidentate HPO ligands were evaluated using an automated spectrophotometric titration system. The pH titration curve for ligand **3** in the presence of iron(III) is presented as an example in Figure 1. A clear shift in λ_{max} is observed in the full speciation spectra of ligand **3**:iron(III) complexes over pH range 1.59-10.05 (Figure 1) which displays the pH dependence of the different metal/ligand equilibrium. At low pH values the λ_{max} of the iron(III) complex (545 nm) corresponds to the $[Fe^{III}L]^{2+}$ complex, and the $[Fe^{III}L_2]^{+}$ complex (λ_{max}, 510 nm) dominates over the pH range 3.0−5.0. Above pH 6.5 the neutral $[Fe^{III}L_3]^{0}$ complex (λ_{max}, 460 nm) is the major species. For bidentate ligands the logarithm of the cumulative stability constants was determined. This value, log β_3, is obtained by summation of the logarithms of three stepwise equilibrium constants (K_1, K_2, and K_3) corresponding to Scheme 8. The optimized values are presented in Table 4. The introduction of a 2-(1′-hydroxyalkyl) substitutent leads to a reduction in both log K values and log β_3 values, as compared with simple alkyl-substituted HPOs (Table 4). The log β_3 values for 2-(1′-hydroxyalkyl) HPOs fall within the range of 34.7−35.6, as compared to 36.4 for CP20 and 36.7 for CP94.

Distribution Coefficients. The distribution coefficients (D) of the ligands between 1-octanol and MOPS buffer (pH 7.4) were determined using an automated filter-probe system.[12,13] Since the degree of ionization of the two functional groups on the pyridinone ring is relatively small at pH 7.4, the neutral species of the compounds is the predominant form (>98%). Hence the distribution coefficients of the compounds at pH 7.4 are expected to be almost identical to their partition coefficients. The resulting values are presented in Table 3. As expected the introduction of a hydroxyl function results in a decrease in lipophilicity relative to the simple alkyl derivatives. The distribution coefficient values of the 2-(1′-hydroxyalkyl) HPOs cover the range 0.048−5.61. The most hydrophobic compound was **21**, the benzoyl ester derivative of **19d**, which possesses a log P value of 0.75.

Iron Mobilization Efficacy in Rats. *In vivo* iron scavenging ability of the 2-(1′-hydroxyalkyl) HPOs was compared with CP20 and CP94 in a [^{59}Fe]ferritin-loaded rat model.[11] All chelators were administered orally, and the dose of chelator was 450 μmol/kg. Several 2-(1′-hydroxymethyl) derivatives such as **19a** and **19f** were found to be poor scavengers of iron under *in vivo* conditions, with efficacies of 4.6% and 0.6%, respectively. However with the substituted 2-(1′-hydroxyalkyl) derivatives, **3**, **19h**, and **19i** were found to be as equally effective as CP94 (Table 5). The benzoyl ester prodrug **21** was also found to be equally effective as CP94. This ester prodrug ($D_{7.4}$ = 5.61) provided a significant improvement in the ability of facilitating iron excretion over that of the parent hydroxyl compound (**19d**) ($D_{7.4}$ = 0.056), the iron mobilization efficacy increasing from 7.8% to 52.1%.

Discussion

In order to understand the greater efficacy of CP94 in rats, the 2-(1′-hydroxyethyl) metabolite of CP94 (**3**) and seven analogues have been synthesized. Both the pK_a values of the ligands and the stability constants of their iron(III) complexes have been evaluated. Generally, simple ring N-alkylation of 3-hydroxypyridin-4-ones results in little change in the affinity for protons as well as for iron(III).[12,13] However 2-alkyl substitution tends to elevate the pK_a values in the order ethyl > methyl > hydrogen[12] by virtue of the positive inductive effect. An additional increment has also been observed with 6-alkyl substitution (unpublished data). However the introduction of a 1′-hydroxyalkyl group at the 2-position significantly reduces the pK_a values (Table 4). This effect results from stabilising the ionised species due to the combined effect of intramolecular hydrogen bonding between the 2-(1′-hydroxyl) group and the adjacent 3-hydroxyl function and the negative inductive effect of the 2-(1′-hydroxyl) group from the pyridinone ring (Figure 2). Although such an effect reduces the overall stability constants for iron(III) (Table 4), it also reduces the affinity of the chelating function for protons. These changes result in an increase in the corresponding pFe^{3+} values at pH 7.4 (Table 4).

In designing iron chelators for clinical application, metal selectivity and ligand-metal complex stability are paramount.[16] The most suitable comparison standard for ligands is the pFe^{3+} value. pFe^{3+} is defined as the negative logarithm of the concentration of the free iron(III) in solution. Typically pFe^{3+} values are calculated for total [ligand] = 10^{-5} M, total [iron] = 10^{-6} M at pH 7.4. The comparison of ligands under these conditions is more meaningful, since pFe^{3+}, unlike the stability constants, takes into account the effects of ligand basicity, ligand protonation, and metal hydrolysis as

Table 3. Synthesis of 2-(1′-Hydroxyalkyl)-3-hydroxypyridin-4-one Hydrochlorides and Their Distribution Coefficients between an Aqueous Phase Buffered at pH 7.4 and Octanol ($n = 5$)

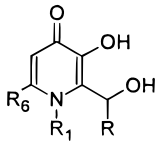

compd	R_1	R	R_6	mp, °C	% yield (from **15**)	formula	anal.	$D_{7.4}$	log *P*
19a	CH_3	H	H	157−159	56.6	$C_7H_{10}NO_3Cl$	C,H,N	0.048 ± 0.003	−1.319
19b	C_2H_5	H	H	168−169	61.4	$C_8H_{12}NO_3Cl$	C,H,N	0.140 ± 0.007	−0.854
3 (19c)	C_2H_5	CH_3	H	139−140	65.5	$C_9H_{14}NO_3Cl$	C,H,N	0.266 ± 0.003	−0.575
19d	$CH_2CH_2CH_2OH$	H	H	138−139	64.7	$C_9H_{14}NO_4Cl$	C,H,N	0.056 ± 0.005	−1.252
19e	$CH_2CH_2CH_2OH$	CH_3	H	117−120	47.2	$C_{10}H_{16}NO_4Cl$	C,H,N	0.075 ± 0.007	−1.125
19f	CH_3	H	CH_3	140−143	57.4	$C_8H_{12}NO_3Cl \cdot {}^1/_2H_2O$	C,H,N	0.098 ± 0.006	−1.009
19g	C_2H_5	H	CH_3	160−162	57.8	$C_9H_{14}NO_3Cl$	C,H,N	0.223 ± 0.018	−0.652
19h	CH_3	CH_3	CH_3	208−212	46.6	$C_9H_{14}NO_3Cl$	C,H,N	0.248 ± 0.012	−0.606
19i	CH_3	C_2H_5	CH_3	221−223	31.7	$C_{10}H_{16}NO_3Cl$	C,H,N	0.734 ± 0.013	−0.134
21	$CH_2CH_2CH_2OOCPh$	H	H	142−143	76.2[a]	$C_{16}H_{18}NO_5Cl$	C,H,N	5.610 ± 0.264	0.749

[a] Percent yield from **18d**.

Table 4. Spectrophotometric and Potentiometric Determined pK_a Values for Ligands and Affinity Constants for Fe(III) Complexes

	pK_{a1}		pK_{a2}		affinity constants for Fe(III)				pFe^{3+}
compd	potentiometric	spectrophotometric	potentiometric	spectrophotometric	log K_1	log K_2	log K_3	log β_3	(at pH 7.45)
CP20	3.68	3.56	9.77	9.64	14.56	12.19	9.69	36.4	19.4
CP94	3.81		9.93		15.20	11.76	9.84	36.8	19.7
19a	2.92	2.93	9.11	9.11	14.47	11.27	9.58	35.3	20.9
19b	2.80	2.88	9.27	9.05	14.66	11.16	9.43	35.3	21.0
3	3.03	3.11	8.77	8.74	15.21	10.97	8.90	35.1	21.4
19d	3.02	2.87	9.29	9.14	15.67	10.01	9.57	35.3	20.7
19e	2.98	2.96	8.72	8.69	14.93	10.87	8.87	34.7	21.5
19f	3.32	3.37	9.44	9.42	14.39	11.57	9.55	35.5	20.4
19g	3.29	3.28	9.45	9.38	14.37	11.60	9.64	35.6	20.4
19h	3.54	3.55	8.99	8.97	15.38	11.09	9.05	35.5	21.5
19i	3.76	3.78	9.00	8.98	14.50	11.48	9.05	35.0	21.0

Scheme 7. Protonation Equilibra of 3-Hydroxypyridin-4-ones

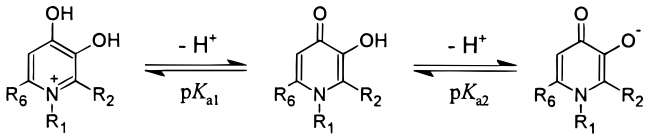

well as differences in metal-ligand stoichiometries. Generally, ligands containing an identical chelating group possess similar pFe^{3+} values: for instance, 3-hydroxypyridin-2-one ligands possess pFe^{3+} values of 16, whereas the pFe^{3+} values for 3-hydroxypyridin-4-ones are around 20.[17] However the introduction of adjacent functions can have a dramatic effect on pFe^{3+} values. It has been previously established that the introduction of an amide function at the 4-position of 3-hydroxypyridin-2-ones reduces the pK_a values and hence increases the pFe^{3+} values, due to the formation of a stable intramolecular hydrogen bond between the amide proton and the adjacent oxygen donor.[18] In this current study, a similar reduction on the pK_a values and hence enhancement on the pFe^{3+} values were also observed by the introduction of a 1′-hydroxyalkyl group at the 2-position of 3-hydroxypyridin-4-ones. Such enhancement on the pFe^{3+} values is typified by CP20 and **19a**, where a differential of almost 1.5 log units in pFe^{3+} values is observed (Table 4). Similarly comparison of CP94 with **3**, which actually is the major metabolite of CP94 in rats, demonstrates a positive increment of 1.7 log units. This difference could account for the extremely high efficacy of CP94 in the rat. In rats CP94 acts as a "prodrug" of **3**, a chelator with a higher pFe^{3+} value.

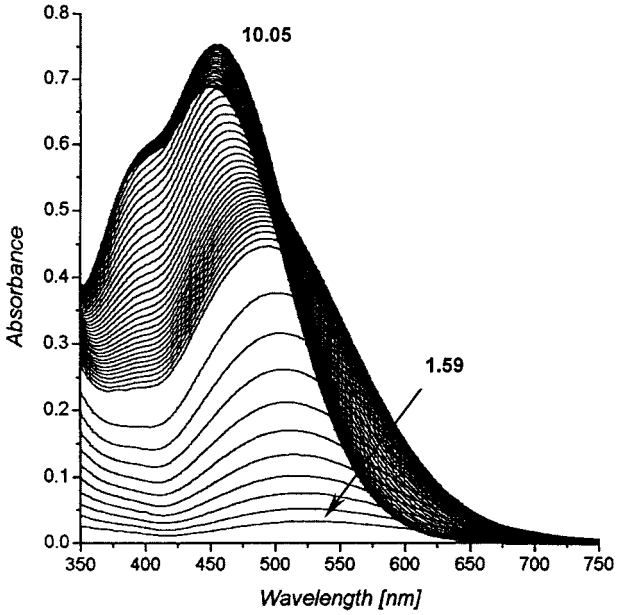

Figure 1. pH dependence of the spectrum of ligand **3** in the presence of iron(III) over the pH range 1.59−10.05: [Fe(III)] = 1.8×10^{-4} M; [**3**] = 1.8×10^{-3} M.

The introduction of a 1′-hydroxyalkyl group at the 2-position also has a dramatic effect on the speciation plot of the iron(III) complexes as presented in Figure 3 which indicates that **3** will dissociate less readily leading

Scheme 8. Complex Formation of Iron(III) with Bidentate 3-Hydroxypyridin-4-ones

$$[Fe^{3+}] + [L^-] \overset{K_1}{\rightleftharpoons} [FeL]^{2+} \qquad K_1 = \frac{[FeL]^{2+}}{[Fe^{3+}][L^-]}$$

$$[FeL]^{2+} + [L^-] \overset{K_2}{\rightleftharpoons} [FeL_2]^{+} \qquad K_2 = \frac{[FeL_2]^{+}}{[FeL]^{2+}[L^-]}$$

$$[FeL_2]^{+} + [L^-] \overset{K_3}{\rightleftharpoons} [FeL_3]^{0} \qquad K_3 = \frac{[FeL_3]^{0}}{[FeL^2]^{+}[L^-]}$$

$$[Fe^{3+}] + 3[L^-] \overset{\beta_3}{\rightleftharpoons} [FeL_3]^{0} \qquad \beta_3 = \frac{[FeL_3]^{0}}{[Fe^{3+}][L^-]^3}$$

Table 5. Iron Mobilization Efficacy Studies of 2-(1′-Hydroxyalkyl)-3-Hydroxypyridin-4-ones in the [^{59}Fe]Ferritin-Loaded Rat Model[a]

chelator	iron mobilization (%)	efficacy (%)
control	3.87 ± 1.0	
19a	8.44 ± 3.6	4.6
19b	33.3 ± 6.7	29.4
3	54.5 ± 9.9	50.6
19d	11.7 ± 4.1	7.8
19e	14.5 ± 4.5	10.6
19f	4.5 ± 1.1	0.6
19g	12.9 ± 2.3	9.0
19h	48.4 ± 7.2	44.5
19i	60.4 ± 15.6	56.5
21	56.0 ± 6.0	52.1

[a] All chelators (450 μmol/kg) were given orally, and control rats were administered with an equivalent volume of water. Values are expressed as means ± SD (n = 5).

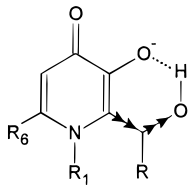

Figure 2. Proposed intramolecular hydrogen bonding between the 2-(1′-hydroxyl) group and the adjacent 3-hydroxyl function and the negative inductive effect of the 2-(1′-hydroxyl) group from the pyridinone ring.

to lower concentrations of the L_2Fe^+ complex compared with CP20. The partial dissociation of iron complexes formed from either bi- or tridentate ligands generates a water-coordinated iron surface which may interact with oxygen and hydrogen peroxide thereby generating hydroxyl radicals.[3] Thus chelators with high pFe^{3+} values are predicted to scavenge iron more effectively at low ligand concentrations and to dissociate less readily, leading to lower concentrations of the partially co-ordinated iron complexes.

In vivo iron mobilization efficacy of this series of compounds has been investigated in the [^{59}Fe]ferritin-labelled rat model. The introduction of a 1′-hydroxymethyl function alone does not improve efficacy; thus **19a** and **19f** are poor scavengers of iron under *in vivo* conditions (Table 5). This may be attributed to the low log P values associated with these molecules (Table 3). Such low lipophilicities may lead to poor oral absorption and liver extraction. Consequently, inefficient iron mobilization would be expected. However with the higher lipophilicities and improved pFe^{3+} values associated with the substituted 2-(1′-hydroxyalkyl) derivatives, **3**, **19h**, and **19i** were found to be as equally effective as CP94. They have a clear advantage over CP94 as their respective log P values, −0.6, −0.59, and −0.14, are significantly lower than that of CP94, namely 0.26. They are therefore predicted to penetrate the blood−brain barrier and the placental barrier and enter peripheral cells (such as the heart and bone marrow) much less readily than CP94. Furthermore these compounds (**3**, **19h**, and **19i**) may not undergo glucuronidation *in vivo* by virtue of the presence of the 1′-hydroxyalkyl function at the 2-position.[5] Such molecules have immense clinical potential for the treatment of iron overload.

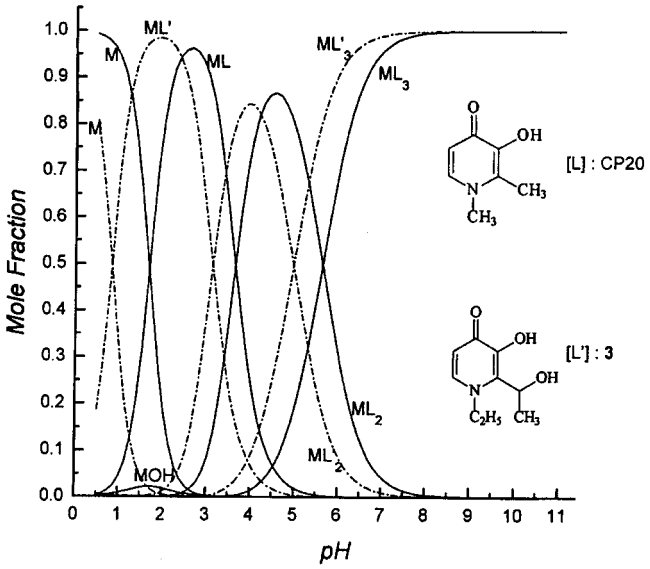

Figure 3. Comparison of the speciation plots between CP20 and **3** in the presence of iron(III): L = CP20; L′ = **3**; [Fe(III)] = 1 × 10^{-6} M; [ligand] = 1 × 10^{-5} M.

In order to improve both drug absorption and hepatic extraction, a benzoyl ester derivative **21** has also been synthesized. This ester prodrug provided a significant improvement in the ability of facilitating iron excretion over that of the parent hydroxyl compound **19d** (Table 5). Such enhancement is almost certainly due to the increased lipophilicity of this ester prodrug as compared to the parent compound, which indicates that selective delivery of the drug to the liver has been achieved (Figure 4). This molecule, due to its relatively high lipophilicity (log P = 0.75), will be expected to be extracted by the liver more efficiently. On entry to the liver, it may undergo rapid hydrolysis to generate the hydrophilic compound **19d** (log P = −1.25) which can be further metabolised to the even more hydrophilic carboxylate metabolite.[10] Such molecules will severely limit the distribution of the chelator, which in turn could possibly minimise the potential toxicity. This ester is the most effective hydroxypyridinone prodrug synthesized to date (Tables 1 and 5).

In summary, the introduction of a 1′-hydroxyalkyl group at the 2-position of 3-hydroxypyridin-4-ones will lead a dramatic enhancement on the pFe^{3+} values. Such novel HPOs show great promise in their ability to remove iron under *in vivo* conditions and thereby may offer a realistic approach to the design of orally active iron chelators for clinical use.

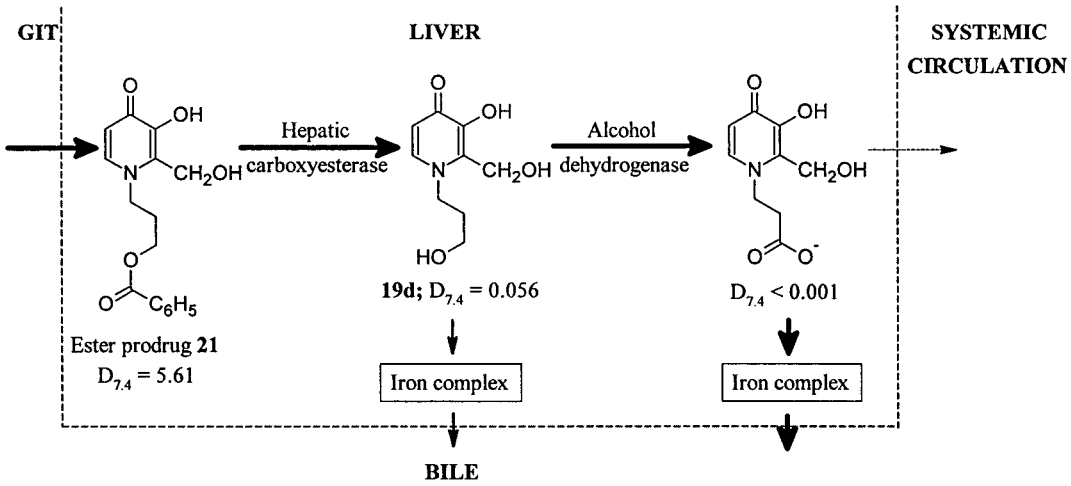

Figure 4. Schematic representation of the use of hydrophobic esters to enhance both the absorption from the gastrointestinal tract (GIT) and the hepatic extraction of the chelator. Subsequent intracellular hydrolysis occurs yielding a hydrophilic chelator which can undergo further metabolism to the extremely hydrophilic negatively charged 1-carboxyalkyl metabolite in the liver.

Experimental Section

General Procedure. Melting points were determined using an Electrothermal IA 9100 digital melting point apparatus and are uncorrected. ^{1}H NMR spectra were recorded using a Perkin-Elmer (60 MHz) NMR spectrometer. Chemical shifts (δ) are reported in ppm downfield from the internal standard tetramethylsilane (TMS). Mass spectra (EI) were recorded on a Joel AX505W. Elemental analyses were performed by Micro Analytical Laboratories, Department of Chemistry, The University of Manchester, Manchester M13 9PL, U.K.

2,5-Dihydro-2,5-dimethoxy-2-furanylmethanol (9). To a solution of furfuryl alcohol (**8**) (98 g, 1.0 mol) in methanol (800 ml) was added sodium hydrogen carbonate (185 g, 2.2 mol), and the mixture was cooled to −30 °C. To this well-stirred solution was added a solution of bromine (176 g, 1.1 mol) in methanol (300 mL). The temperature of the reaction was maintained between −30 and −10 °C. After the addition period the reaction mixture was allowed to warm to room temperature and stirred for 2 h. The reaction was then filtered and concentrated. The residue was taken up into toluene (300 mL) and filtered through aluminium oxide. Evaporation of the solvent and distillation at 74 °C/0.4 mmHg (lit. value[19] 71 °C/1.0 mmHg) gave a colorless liquid (115.5g, 72.2%). ^{1}H NMR ($CDCl_3$) δ: 2.33 (br, s, 1H, CH_2**OH**), [3.25 (s, isomer A) & 3.3 (s, isomer B), 3H, **5-OCH$_3$**], 3.6 (s, 3H, **2-OCH$_3$**), 3.7 (br, s, 2H, **CH$_2$**OH), [5.55 (s, isomer B) & 5.8 (s, isomer A), 1H, **5-H**], 5.9-6.4 (m, 2H, **3,4-H**).

6-Methoxy-2*H*-pyran-3(6*H*)-one (10). A solution of **9** (80 g, 0.5 mol) in methanol (30 mL) was added during 15 min at 25 °C to a well-stirred solution of methanol (20 mL) in formic acid (400 mL). The mixture was then poured into water (1000 mL) and extracted with chloroform (3 x 500 mL). The extracts were combined, washed successively with saturated sodium hydrogen carbonate solution and brine, dried with anhydrous sodium sulfate, and concentrated *in vacuo* to yield a light brown oil (54g, 84.4%). Distillation at 47−48 °C/0.5 mmHg (lit. value[19] 76−81 °C/13 mmHg) afforded a clear, sharp-smelling oil. ^{1}H NMR ($CDCl_3$) δ: 3.5 (s, 3H, **OCH$_3$**), 4.18 (q, 2H, **2,2′-H**, AB center, $J_{22'}$ = 16.5 Hz, $\Delta\delta_{22'}$ = 20.5 Hz), 5.02 (d, 1H, **6-H**), 6.03 (d, 1H, **4-H**), 6.81 (q, 1H, **5-H**, J_{56} = 3.3 Hz, J_{45} = 10.2 Hz).

4-Bromo-6-methoxy-2*H*-pyran-3(6*H*)-one (11). To a solution of **10** (12.8 g, 0.1 mol) in dichloromethane (40 mL) at 0 °C was added 16.0 g (0.1 mol) of bromine in dichloromethane (10 mL). Then triethylamine (14 mL) was added dropwise at 0 °C and the reaction was allowed to warm to room temperature and stirred for 2 h. The reaction was then diluted with toluene (200 mL). After filtration, the organic solution was then washed with 5% sodium hydrogen carbonate solution and brine, dried with anhydrous sodium sulfate, filtered, and concentrated to yield the crude product as a light brown solid. Recrystallization from ethyl acetate afforded a white crystalline solid (17g, 82%): mp 74−75 °C. ^{1}H NMR ($CDCl_3$) δ: 3.5 (s, 3H, **OCH$_3$**), 4.4 (q, 2H, **2,2′-H**, AB center, $J_{22'}$ = 14.5 Hz, $\Delta\delta_{22'}$ = 18.5 Hz), 5.05 (d, 1H, **6-H**), 7.25 (d, 1H, **5-H**). MS (EI): *m*/*z* 207 [$M^{+\bullet}$]. Anal. ($C_6H_7O_3Br$) C, H.

3-Hydroxypyran-4(1*H*)-one (Pyromeconic acid) (12). 5.8 g (28 mmol) of **11** was added to trifluoroacetic acid (30 mL) and refluxed for 2 h. Concentration to dryness *in vacuo* followed by repeated re-evaporations from methanol afforded a brown crystalline residue. The solid was treated with activated carbon and recrystallized from toluene to yield light yellow plates (2.5 g, 80%): mp 114−115 °C (lit. value[20] 113−115.5 °C). ^{1}H NMR ($CDCl_3$) δ: 6.48 (d, 1H, **5-H**), 6.3−7.4 (br, 1H, **OH**), 7.76 (d, 1H, **6-H**), 7.88 (s, 1H, **2-H**).

2-Methyl-5-hydroxypyran-4(1*H*)-one (allomaltol) (15) was synthesized from kojic acid (**13**) in two steps using the established procedure.[21]

2-Hydroxymethyl-3-hydroxypyran-4(1*H*)-one (16a). Sodium hydroxide (4 g, 100 mmol) dissolved in distilled water (10 mL) was added to a solution of **12** (8.96 g, 80 mmol, 1 equiv) in methanol (50 mL) and allowed to stir at room temperature for 5 min; 35% formaldehyde solution (16 mL) was added dropwise over 15 min and the solution was stirred overnight. After adjustment to pH 1 with 37% hydrochloric acid, the reaction mixture was concentrated *in vacuo* to dryness and the resulting solid was extracted with isopropanol (2 × 100 mL) at 90 °C. The isopropanol extracts were concentrated to yield the crude products. Recrystallization from isopropanol afforded a white crystalline solid (9.7 g, 85.4%): mp 154−156 °C (lit. value[20] 154−155 °C). ^{1}H NMR (DMSO-d_6) δ: 4.4 (s, 2H, 2-**CH$_2$**OH), 4.6−5.7 (br, 1H, 2-CH$_2$**OH**), 6.34 (d, 1H, **5-H**), 8.1 (d, 1H, **6-H**), 9.0 (br, s, 1H, **3-OH**).

2-(1′-Hydroxyethyl)-3-hydroxypyran-4(1*H*)-one (16b). Pyromeconic acid (**12**) (5.6 g, 50 mmol) was added to water (50 mL) and the pH of the solution was adjusted to 10.5 using 50% aqueous sodium hydroxides. Acetaldehyde (2.64 g, 60 mmol) dissolved in water (20 mL) was slowly added dropwise over 1 h and the solution allowed to stir overnight. The reaction mixture was acidified to pH 1 with 37% hydrochloric acid and concentrated *in vacuo* to dryness. The residue was extracted with isopropanol (2 × 70 mL) at 90 °C. The isopropanol extracts were combined and concentrated to yield, after recrystallization from toluene, a pale yellow crystalline solid (3.7 g, 47.4%): mp 131−132 °C (lit. value[20] 130−131 °C). ^{1}H NMR (DMSO-d_6) δ: 1.3 (d, 3H, 2-CH**CH$_3$**), 5.03 (q, 1H, 2-**CH**CH$_3$), 6.38 (d, 1H, **5-H**), 8.2 (d, 1H, **6-H**).

2-Hydroxymethyl-3-hydroxy-6-methylpyran-4(1*H*)-one (16c), 2-(1′-hydroxyethyl)-3-hydroxy-6-methylpyran-4(1*H*)-one (16d), and 2-(1′-hydroxypropyl)-3-hydroxy-6-

methylpyran-4(1*H*)-one (16e) were synthesized from allomaltol (**15**) by following the methodology as described by Ellis et al.[21]

8-Oxo-4,8-dihydro-2-phenyl-4*H*-pyrano[3,2-*d*]-*m*-dioxin (17a). A solution of **16a** (2.84 g, 20 mmol), benzaldehyde dimethyl acetal (6.08 g, 40 mmol), and toluene-*p*-sulfonic acid monohydrate (0.04g, cat.) in *N*,*N*-dimethylformamide (50 mL) was rotated under aspirator pressure at 80 °C for 3 h. The solvent was removed under high vacuum and the residue taken up into dichloromethane (100 mL). The organic solution was washed successively with 5% sodium hydrogen carbonate solution and brine. After drying over magnesium sulfate, the solvent was removed to give the crude product. Recrystallization form dichloromethane/petroleum ether (40−60 °C) afforded a white crystalline solid (3.77 g, 82%): mp 141−143 °C. ^{1}H NMR ($CDCl_3$) δ: 4.7 (d, 2H, **CH$_2$**O), 5.88 (s, 1H, **CH**Ph), 6.35 (d, 1H, **7-H**(pyranone)), 7.2−7.9 (m, 6H, **Ar** & **6-H**(pyranone)); MS (EI): *m*/*z*, 230 [M$^{+\bullet}$]. Anal. ($C_{13}H_{10}O_4$) C, H.

Analogous syntheses starting with **16b**−**16e** gave compounds **17b**−**17e** as shown in Table 2.

8-Oxo-4,8-dihydro-4-methyl-2-phenyl-4*H*-pyrano[3,2-*d*]-*m*-dioxin (17b): mp 112−113 °C. ^{1}H NMR ($CDCl_3$) δ: 1.55 (d, 3H, CH**CH$_3$**), 5.0 (q, 1H, **CH**CH$_3$), 5.8 (s, 1H, **CH**Ph), 6.25 (d, 1H, **7-H**(pyranone)), 7.1−7.75 (m, 6H, **Ar** & **6-H**(pyranone)). MS (EI): *m*/*z* 244 [M$^{+\bullet}$]. Anal. ($C_{14}H_{12}O_4$) C, H.

8-Oxo-4,8-dihydro-6-methyl-2-phenyl-4*H*-pyrano[3,2-*d*]-*m*-dioxin (17c): mp 91−94 °C. ^{1}H NMR ($CDCl_3$) δ: 2.25 (s, 3H, **6-CH$_3$**), 4.75 (d, 2H, **CH$_2$**O), 5.9 (s, 1H, **CH**Ph), 6.18 (s, 1H, **7-H**(pyranone)), 7.2−7.8 (m, 5H, **Ar**). MS (EI): *m*/*z* 244 [M$^{+\bullet}$]. Anal. ($C_{14}H_{12}O_4$) C, H.

8-Oxo-4,8-dihydro-4,6-dimethyl-2-phenyl-4*H*-pyrano-[3,2-*d*]-*m*-dioxin (17d): mp 120−122 °C. ^{1}H NMR ($CDCl_3$) δ: 1.6 (d, 3H, CH**CH$_3$**), 2.25 (s, 3H, **6-CH$_3$**), 5.08 (q, 1H, **CH**CH$_3$), 5.9 (s, 1H, **CH**Ph), 6.18 (s, 1H, **7-H**(pyranone)), 7.2−7.8 (m, 5H, **Ar**). MS (EI): *m*/*z* 258 [M$^{+\bullet}$]. Anal. ($C_{15}H_{14}O_4$) C, H.

8-Oxo-4,8-dihydro-4-ethyl-6-methyl-2-phenyl-4*H*-pyrano[3,2-*d*]-*m*-dioxin (17e): mp 111−114 °C. ^{1}H NMR ($CDCl_3$) δ: 1.0 (t, 3H, CHCH$_2$**CH$_3$**), 1.6−2.1 (m, 2H, CH**CH$_2$**CH$_3$), 2.2 (s, 3H, **6-CH$_3$**), 4.7−5.0 (m, 1H, **CH**CH$_2$CH$_3$), 5.8 (s, 1H, **CH**Ph), 6.1 (s, 1H, **7-H** (pyranone)), 7.15−7.7 (m, 5H, **Ar**). MS (EI): *m*/*z* 272 [M$^{+\bullet}$]. Anal. ($C_{16}H_{16}O_4$) C, H.

8-Oxo-4,8-dihydro-2-phenyl-5-methyl-4*H*-pyridino[3,2-*d*]-*m*-dioxin (18a). To a solution of **17a** (2.3 g, 10 mmol) in ethanol (10 mL)/water (10 mL) was added 40% aqueous methylamine (2.5 mL) followed by 2 N sodium hydroxide solution until pH 12.5 was obtained. The reaction mixture was sealed in a thick-walled glass tube and stirred at 70 °C for 3 h. After adjustment to pH 1 with concentrated hydrochloric acid, the solvent was removed by rotary evaporation prior to addition of water (50 mL) and washing with diethyl ether (3 × 50 mL). Subsequent adjustment of the aqueous fraction to pH 7 with 10 N sodium hydroxide solution was followed by extraction into dichloromethane (4 × 50 mL), the combined organic layers then being dried over anhydrous sodium sulfate, filtered, and rotary-evaporated to give a yellow solid. Recrystallization from methanol/diethyl ether afforded a light yellow crystalline solid (1.6 g, 65.8%): mp 210−211 °C. ^{1}H NMR (DMSO-d_6) δ: 3.55 (s, 3H, N-**CH$_3$**), 5.08 (s, 2H, **CH$_2$**O), 5.92 (s, 1H, **CH**Ph), 6.12 (d, 1H, **7-H**(pyridinone)), 7.25-7.85 (m, 6H, **Ar** & **6-H**(pyridinone)).

Analogous syntheses starting with reaction of **17a**−**17e** with methylamine or ethylamine gave compounds **18b**, **18c**, and **18f**−**18i** as shown in Table 2.

8-Oxo-4,8-dihydro-2-phenyl-5-ethyl-4*H*-pyridino[3,2-*d*]-*m*-dioxin (18b): purification by column chromatography on silica gel (eluant: methanol:chloroform, 15:85 v/v) (69.7%); mp 177−179 °C. ^{1}H NMR (DMSO-d_6) δ: 1.3 (t, 3H, N-CH$_2$**CH$_3$**), 3.8 (q, 2H, N-**CH$_2$**CH$_3$), 5.12 (s, 2H, **CH$_2$**O), 5.9 (s, 1H, **CH**Ph), 6.25 (d, 1H, **7-H** (pyridinone)), 7.1-7.8 (m, 6H, **Ar** & **6-H**(pyridinone)).

8-Oxo-4,8-dihydro-2-phenyl-4-methyl-5-ethyl-4*H*-pyridino[3,2-d]-*m*-dioxin (18c): purification by column chromatography on silica gel (eluant:methanol:chloroform, 15:85 v/v) to afford a yellow oil (79.1%). ^{1}H NMR ($CDCl_3$) δ: 1.2−2.2 (m, 6H, CH**CH$_3$** & N-CH$_2$**CH$_3$**), 3.4−4.0 (m, 2H, N-**CH$_2$**CH$_3$), 4.8−5.4 (m, 1H, **CH**CH$_3$), [5.6 (s, isomer A) & 6.0 (s, isomer B); 1H, **CH**Ph], 6.3 (d, 1H, **7-H**(pyridinone)), 7.0−7.7 (m, 6H, **Ar** & **6-H**(pyridinone)).

8-Oxo-4,8-dihydro-2-phenyl-5,6-dimethyl-4*H*-pyridino-[3,2-*d*]-*m*-dioxin (18f): 66%; mp 256−258 °C. ^{1}H NMR (methanol-d_4) δ: 2.2 (s, 3H, 6-**CH$_3$**), 3.35 (s, 3H, N-**CH$_3$**), 4.95 (s, 2H, **CH$_2$**O), 5.8 (s, 1H, **CH**Ph), 6.5 (s, 1H, **7-H**(pyridinone)), 7.0−7.5 (m, 5H, **Ar**).

8-Oxo-4,8-dihydro-2-phenyl-5-ethyl-6-methyl-4*H*-pyridino[3,2-*d*]-*m*-dioxin (18g): purification by column chromatography on silica gel (eluant:methanol:chloroform, 20:80 v/v) (62.3%); mp 201−203 °C. ^{1}H NMR (DMSO-d_6) δ: 1.25 (t, 3H, N-CH$_2$**CH$_3$**), 2.3 (s, 3H, 6-**CH$_3$**), 3.85 (q, 2H, N-**CH$_2$**CH$_3$), 5.02 (s, 2H, **CH$_2$**O), 5.9 (s, 1H, **CH**Ph), 6.45 (d, 1H, **7-H** (pyridinone)), 7.1−7.6 (m, 5H, **Ar**).

8-Oxo-4,8-dihydro-2-phenyl-4,5,6-trimethyl-4*H*-pyridino-[3,2-*d*]-*m*-dioxin (18h): purification by column chromatography on silica gel (eluant:methanol:chloroform, 20:80 v/v) (56.8%); mp 199−201 °C. ^{1}H NMR (DMSO-d_6) δ: 1.7 (dd, 3H, CH**CH$_3$**), 2.35 (s, 3H, 6-**CH$_3$**), [3.44 (s, isomer B) & 3.5 (s, isomer A), 3H, N-**CH$_3$**], 4.9−5.4 (m, 1H, **CH**CH$_3$), [5.75 (s, isomer A) & 6.05 (s, isomer B), 1H, **CH**Ph], 6.35 (s, 1H, **7-H**(pyridinone)), 7.2-7.9 (m, 5H, **Ar**).

8-Oxo-4,8-dihydro-2-phenyl-4-ethyl-5,6-dimethyl-4*H*-pyridino[3,2-*d*]-*m*-dioxin (18i): purification by column chromatography on silica gel (eluant:methanol:chloroform, 20:80 v/v) (39.8%); mp 185−187 °C. ^{1}H NMR (DMSO-d_6) δ: 0.8−1.4 (m, 3H, CHCH$_2$**CH$_3$**), 1.5−2.2 (m, 2H, CH**CH$_2$**CH$_3$), 2.3 (s, 3H, **6-CH$_3$**), [3.38 (s, isomer B) & 3.45 (s, isomer A), 3H, N-**CH$_3$**], [4.5−4.8 (m, isomer B) & 4.9−5.4 (m, isomer A), 1H, **CH**CH$_2$-CH$_3$], [5.68 (s, isomer A) & 5.95 (s, isomer B), 1H, **CH**Ph], 6.25 (s, 1H, **7-H**(pyridinone)), 7.2−7.8 (m, 5H, **Ar**).

8-Oxo-4,8-dihydro-2-phenyl-5-(3′-hydroxypropyl)-4*H*-pyridino[3,2-*d*]-*m*-dioxin (18d). To a solution of **17a** (3.45 g, 15 mmol) in ethanol (50 mL)/water (50 mL) was added 3-amino-1-propanol (2.25 g, 30 mmol) followed by 2 N sodium hydroxide solution until pH 12.5 was obtained. The reaction mixture was refluxed for 3 h. TLC analysis (eluant:methanol: chloroform, 10:90 v/v) showed that no starting material was present. After removal of solvent by rotary evaporation, the residue was purified by column chromatography on silica gel (eluant:methanol:chloroform, 20:80 v/v) to afford a yellow crystalline solid (3.35 g, 77.8%): mp 73−76 °C, ^{1}H NMR ($CDCl_3$) δ: 1.5−2.1 (m, 2H, N-CH$_2$**CH$_2$**CH$_2$O), 3.2−4.0 (m, 4H, N-**CH$_2$**CH$_2$**CH$_2$**O), 4.0−5.2 (br, 1H, **OH**), 4.8 (s, 2H, **CH$_2$**O), 5.7 (s, 1H, **CH**Ph), 6.2 (d, 1H, **7-H**(pyridinone)), 7.0−7.8 (m, 6H, **Ar** & **6-H**(pyridinone)).

Analogous reaction of **17b** gave compound **18e** (Table 2).

8-Oxo-4,8-dihydro-2-phenyl-4-methyl-5-(3′-hydroxypropyl)-4*H*-pyridino [3,2-*d*]-*m*-dioxin (18e): 57.6%; oil. ^{1}H NMR ($CDCl_3$) δ: 1.5 (d, 3H, CH**CH$_3$**), 1.5−2.1 (m, 2H, NCH$_2$**CH$_2$**CH$_2$O), 3.2−4.0 (m, 4H, N**CH$_2$**CH$_2$**CH$_2$**O), 4.0−5.2 (br, 1H, **OH**), 5.28 (q, 1H, **CH**CH$_3$), 5.58 (s, 1H, **CH**Ph), 6.2 (d, 1H, **7-H**(pyridinone)), 7.0−7.8 (m, 6H, **Ar** & **6-H**(pyridinone)).

1-Methyl-2-hydroxymethyl-3-hydroxypyridin-4(1*H*)-one Hydrochloride (19a). A solution of **18a** (1.22 g, 5mmol) in ethanol (30 mL) was adjusted to pH 1 with concentrated hydrochloric acid prior to hydrogenolysis for 12 hours in the presence of 5% Pd/C catalyst (0.2g). Filtration followed by rotary evaporation gave the crude product as a white solid. Recrystallization from methanol/diethyl ether gave a white crystalline solid (0.82 g, 86%): mp 157−159 °C. ^{1}H NMR (DMSO-d_6) δ: 4.18 (s, 3H, **N-CH$_3$**), 4.8 (s, 2H, 2-**CH$_2$**OH), 7.4 (d, 1H, **5-H**(pyridinone)), 8.3 (d, 1H, **6-H** (pyridinone)), 7.6−9.3 (br, 3H, **OH**). MS (EI): *m*/*z* 156 [(M − Cl)$^{+\bullet}$]. Anal. (C_7H_{10}-NO_3Cl) C, H, N.

Analogous reaction of **18b**−**18i** gave compounds **19b**−**19i**, respectively, as shown in Table 3.

1-Ethyl-2-hydroxymethyl-3-hydroxypyridin-4(1*H*)-one hydrochloride (19b): 73%; mp 168−169 °C. ^{1}H NMR (D_2O) δ: 1.45 (t, 3H, N-CH$_2$**CH$_3$**), 4.4 (q, 2H, N-**CH$_2$**CH$_3$), 4.88

(s, 2H, 2-**CH$_2$**O), 7.1 (d, 1H, **5-H**(pyridinone)), 8.1 (d, 1H, **6-H** (pyridinone)). MS (EI): *m/z*, 170 [(M − Cl)$^{+\bullet}$]. Anal. ($C_8H_{12}NO_3Cl$) C, H, N.

1-Ethyl-2-(1′-hydroxyethyl)-3-hydroxypyridin-4(1*H*)-one hydrochloride (3) (19c): 82.8%; mp 139−140 °C. ^{1}H NMR (DMSO-d_6) δ: 1.3−1.9 (m, 6H, CH**CH$_3$** & N-CH$_2$**CH$_3$**, 4.6 (q, 2H, N-**CH$_2$**CH$_3$), 5.55 (q, 1H, **CH**CH$_3$), 7.4 (d, 1H, **5-H**(pyridinone)), 8.25 (d, 1H, **5-H**(pyridinone)), 8.5−10.5 (br, 3H, **OH**). MS (EI): *m/z* 184 [(M − Cl)$^{+\bullet}$]. Anal. ($C_9H_{14}NO_3Cl$) C, H, N.

1-(3′-Hydroxypropyl)-2-hydroxymethyl-3-hydroxypyridin-4(1*H*)-one hydrochloride (19d): 83.2%; mp 138−139 °C. ^{1}H NMR (D_2O) δ: 1.9−2.6 (m, 2H, N-CH$_2$**CH$_2$**CH$_2$O), 3.75 (t, 2H, N-CH$_2$CH$_2$**CH$_2$**O), 4.6 (m, 4H, N-**CH$_2$**CH$_2$CH$_2$O), 5.08 (s, 2H, **CH$_2$**O), 7.25 (d, 1H, **5-H**(pyridinone)), 8.2 (d, 1H, **6-H**(pyridinone)). MS (EI): *m/z* 200 [(M − Cl)$^{+\bullet}$]. Anal. ($C_9H_{14}NO_4Cl$) C, H, N.

1-(3′-Hydroxypropyl)-2-(1′-hydroxyethyl)-3-hydroxypyridin-4(1*H*)-one hydrochloride (19e): 82%; mp 117−120 °C. ^{1}H NMR (DMSO-d_6) δ: 1.5 (d, 3H, CH**CH$_3$**), 1.65−2.45 (m, 2H, N-CH$_2$**CH$_2$**CH$_2$O), 3.45 (t, 2H, N-CH$_2$CH$_2$**CH$_2$**O), 4.65 (m, 4H, N-**CH$_2$**CH$_2$CH$_2$O), 5.5 (s, 2H, **CH**CH$_3$), 7.3 (d, 1H, **5-H**(pyridinone)), 8.18 (d, 1H, **6-H**(pyridinone)), 7.3−9.4 (br, 4H, **OH**). MS (EI): *m/z* 214 [(M − Cl)$^{+\bullet}$]. Anal. ($C_{10}H_{16}NO_4Cl$) C, H, N.

1,6-Dimethyl-2-hydroxymethyl-3-hydroxypyridin-4(1*H*)-one hydrochloride (19f): 87.5%; mp 140−143 °C. ^{1}H NMR (DMSO-d_6) δ: 2.7 (s, 3H, **6-CH$_3$**), 4.06 (s, 3H, **N-CH$_3$**), 4.86 (s, 2H, 2-**CH$_2$**OH), 7.4 (s, 1H, **5-H**(pyridinone)), 6.4−8.7 (br, 3H, **OH**). MS (EI): *m/z* 170 [(M − Cl)$^{+\bullet}$]. Anal. ($C_8H_{12}NO_3Cl\cdot{}^1/_2H_2O$) C, H, N.

1-Ethyl-2-hydroxymethyl-3-hydroxy-6-methylpyridin-4(1*H*)-one hydrochloride (19g): 85%; mp 160−162 °C. ^{1}H NMR (DMSO-d_6) δ: 1.3 (t, 3H, N-CH$_2$**CH$_3$**), 2.5 (s, 3H, **6-CH$_3$**), 4.3 (q, 2H, N-**CH$_2$**CH$_3$), 4.6 (s, 2H, 2-**CH$_2$**O), 7.1 (s, 1H, **5-H**(pyridinone)), 7.8−10.0 (br, **OH**). MS (EI): *m/z* 184 [(M − Cl)$^{+\bullet}$]. Anal. ($C_9H_{14}NO_3Cl$) C, H, N.

1,6-Dimethyl-2-(1′-hydroxyethyl)-3-hydroxypyridin-4(1*H*)-one hydrochloride (19h): 82%; mp 208−212 °C. ^{1}H NMR (DMSO-d_6) δ: 1.4 (d, 3H, CH**CH$_3$**), 2.5 (s, 3H, **6-CH$_3$**), 4.04 (s, 3H, **N-CH$_3$**), 5.65 (q, 1H, **CH**CH$_3$), 7.3 (s, 1H, **5-H**(pyridinone)), 7.5−10.0 (br, 3H, **OH**). MS (EI): *m/z* 184 [(M − Cl)$^{+\bullet}$]. Anal. ($C_9H_{14}NO_3Cl$) C, H, N.

1,6-Dimethyl-2-(1′-hydroxypropyl)-3-hydroxypyridin-4(1*H*)-one hydrochloride (19i): 79.7%; mp 221−223 °C. ^{1}H NMR (DMSO-d_6) δ: 0.8 (t, 3H, CHCH$_2$**CH$_3$**), 1.3−2.1 (m, 2H, CH**CH$_2$**CH$_3$), 2.43 (s, 3H, **6-CH$_3$**), 3.94 (s, 3H, **N-CH$_3$**), 5.3 (t, 1H, **CH**CH$_2$CH$_3$), 7.15 (s, 1H, **5-H**(pyridinone)), 7.5−10.5 (br, 3H, **OH**). MS (EI): *m/z* 198 [(M − Cl)$^{+\bullet}$]. Anal. ($C_{10}H_{16}NO_3Cl$) C, H, N.

8-Oxo-4,8-dihydro-2-phenyl-5-[3′-benzoyloxy)propyl]-4*H*-pyridino[3,2-*d*]-*m*-dioxin (20). A solution of triphenylphosphine (3.46 g, 13.2 mmol) and **18d** (3.3 g, 12 mmol) in dry tetrahydrofuran (100 mL) was added dropwise to a solution of diethyl azodicarboxylate (2.3 g, 13.2 mmol) and benzoic acid (1.5 g, 12 mmol) in dry tetrahydrofuran (30 mL) at room temperature. After the mixture stirred overnight at room temperature, the solvent was removed under reduced pressure. The residue thus obtained was purified by column chromatography on silica gel (eluant:methanol:chloroform, 12:88 v/v) yielding a light yellow oil (4.1 g, 89.7%). ^{1}H NMR ($CDCl_3$) δ: 1.95−2.55 (m, 2H, N-CH$_2$**CH$_2$**CH$_2$O), 3.82 (t, 2H, N-**CH$_2$**CH$_2$-CH$_2$O), 4.34 (t, 2H, N-CH$_2$CH$_2$**CH$_2$**O), 4.9 (s, 2H, **CH$_2$**O), 5.8 (s, 1H, **CH**Ph), 6.3 (d, 1H, **7-H**(pyridinone)), 7.0-8.2 (m, 11H, **Ar** & **6-H**(pyridinone)).

1-[(3′-(Benzoyloxy)propyl]-2-hydroxymethyl-3-hydroxypyridin-4(1*H*)-one Hydrochloride (21). A solution of **20** (4.1 g, 10 mmol) in *N,N*-dimethylformamide (50 mL) was adjusted to pH 1 with concentrated hydrochloric acid prior to hydrogenolysis for 6 h in the presence of 5% Pd/C catalyst (1.0g). Filtration followed by rotary evaporation *in vacuo* gave a white solid. Recrystallization from methanol/diethyl ether gave a white crystalline solid (2.9 g, 85%): mp 142−143 °C. ^{1}H NMR (DMSO-d_6) δ: 1.9−2.8 (m, 2H, N-CH$_2$**CH$_2$**CH$_2$O), 4.0−5.0 (m, 4H, N-**CH$_2$**CH$_2$**CH$_2$**O), 4.8 (s, 2H, **CH$_2$**O), 7.2−8.1 (m, 6H, **Ar** & **5-H**(pyridinone)), 8.3 (d, 1H, **6-H**(pyridinone)), 8.5−10.2 (br, 3H, **OH**). MS (EI): *m/z* 304 [(M − Cl)$^{+\bullet}$]. Anal. ($C_{16}H_{18}NO_5Cl$) C, H, N.

Determination of Physicochemical Properties of Ligands. 1. pK_a Determination. Equilibrium constants of protonated ligands were determined using an automated computerized system, consisting of a Metrohm 665 dosimat, a Perkin-Elmer Lambda 5 UV/vis spectrophotometer, a Corning Delta 225 pH meter, and a 286 Opus PC which controlled the integrated system.[22] A combined Sirius electrode was used to calibrate the electrode zero and to measure pH values. This system is capable of undertaking simultaneous potentiometric and spectrophotometric measurements. A blank titration of 0.1 M KCl (25 mL) was carried out to determine the electrode zero using Gran's plot method.[23] The solution (0.1 M KCl, 25 mL), contained in a jacketed titration cell, was acidified by 0.15 mL of 0.2 M HCl. Titrations were carried out against 0.3 mL of 0.2 M KOH using 0.01-mL increments dispensed from the dosimat. Solutions were maintained at 25 ± 0.5 °C under an argon atmosphere. The above titration was repeated in the presence of ligand. The data obtained from titrations were subjected to non-linear least-square regression analysis using the NONLINM1 program.[22] The pK_a values were obtained to an accuracy of ±0.02 pH unit.

2. Iron(III) Affinity Constant Determination. The stability constants were optimized from the spectrophotometric titration of the metal−ligand system using the pK_a values, electrode slope, and electrode zero determined above. The analytical equipment used was similar to that used for pK_a determination. The electrodes were calibrated by titrating a volumetric standard strong acid with a volumetric standard strong base under argon gas. In order to maintain sufficient sensitivity, a 10-mm UV flow-cell was utilised. After electrode calibration, the solution was reacidified by adding concentrated hydrochloric acid and the pH of the solution was adjusted to 1.5-2.0. Iron(III) stock solution (atomic absorption standard; Aldrich) and the test ligand were then added to give a final ligand:iron(III) ratio of about 10:1. A preadjusted programmed autoburette was used for the addition of a 0.2 M KOH solution. The resulting spectrophotometric titration curve was then subjected to non-linear least-square regression analysis.[22]

3. Determination of Distribution Coefficients. Distribution coefficients were determined using an automated continuous flow technique.[12,13] The system comprised an IBM compatible PC running the Omniferous Personal Computer Auto-Titrator "TOPCAT" program, which controlled both a Metrohm 665 dosimat autoburette and a Pye-Unicam Lambda 5 UV/vis spectrophotometer, as well as performing all calculations of distribution coefficients. All distribution coefficient determinations were performed using AnalaR grade reagents under a nitrogen atmosphere using a flat-based glass vessel equipped with a sealable lid at 25 °C. The aqueous and octanol phases were presaturated with respect to each other before use. The filter probe consisted of a polytetrafluoroethylene (PTFE) plunger associated with a gel-filtration column. The aqueous phase (50 mM MOPS buffer, pH 7.4, prepared using Milli-Q water) was separated from the two-phase system (1-octanol/MOPS buffer, pH 7.4) by means of a hydrophilic cellulose filter (5 μm diameter, 589/3 Blauband filter paper; Schleicher and Schuell) mounted in the gel-filtration column adjuster (SR 25/50, Pharmacia). A known volume (normally 25−50 mL) of MOPS buffer (saturated with octanol) is taken in the flat base mixing chamber. After a base line was obtained the solution was used for reference absorbance. The compound to be examined was dissolved in buffer (saturated with octanol) so as to give an absorbance of between 0.5−1.5 absorbance units at the preselected wavelength (∼280 nm). The flow rate of the aqueous circuit was limited to 1 mL. The computer program calculates the distribution coefficient ($D_{7.4}$) for each octanol addition.

Biological Method: Iron Mobilization Efficacy Study in [^{59}Fe]Ferritin-Loaded Rats. Hepatocytes of normal fasted rats (190−230 g) were labelled with ^{59}Fe by administration of [^{59}Fe]ferritin from tail vein.[11] One hour later, each rat was

administered orally with chelator (450 μmol/kg). Control rats were administered with an equivalent volume of water. The rats were placed in individual metabolic cages and urine and feces collected. Rats were allowed access to food one hour after oral administration of chelator. There was no restriction of water throughout the study period. The investigation was terminated 24 h after the [^{59}Fe]ferritin administration, rats were sacrificed, and the liver and gastrointestinal tract (including its content and feces) were removed for gamma counting. The "iron mobilization" and "efficacy" were calculated according to following equations:

$$\text{iron mobilization (\%)} = \frac{^{59}\text{Fe-activity}_{(\text{gut\&feces})}}{^{59}\text{Fe-activity}_{(\text{gut\&feces})} + {}^{59}\text{Fe-activity}_{(\text{liver})}} \times 100\% \quad (1)$$

$$\text{efficacy (\%)} = \text{iron mobilization (\%)} - \text{control (\%)} \quad (2)$$

Acknowledgment. The authors thank Apotex Research Inc., Canada, and Biomed EC Grant BMH4-CT97-2149 for supporting this research project.

References

(1) Brittenham, G.M. Disorders of iron metabolism: deficiency and overload. In *Hematology: Basic Principles and Practice*; Hoffman, R., Benz, E., Shattil, S., Furie, B., Cohen, H., Eds.; Churchill Livingstone: New York, 1991; pp 327−349.
(2) Hershko, C.; Konijn A.M.; Link, G. Iron chelators for thalasaemia. *Br. J. Haematol.* **1998**, *101*, 399−406.
(3) Tilbrook, G. S.; Hider, R.C. Iron Chelators for clinical use. In *Metal Irons in Biological Systems. Vol. 35: Iron Transport and Storage in Microorganisms, Plants and Animals*; Sigel, A., Sigel, H., Eds.; Marcel Dekker: New York, 1998; pp 691−730.
(4) Brittenham, G. M. Development of iron-chelating agents for clinical use. *Blood* **1992**, *80*, 569−574.
(5) Singh, S.; Epemolu, O.; Dobbin, P. S.; Tilbrook, G. S.; Ellis, B. L.; Damani, L. A.; Hider, R. C. Urinary metabolic profiles in man and rat of 1,2-dimethyl- and 1,2-diethyl substituted 3-hydroxypyridin-4-ones. *Drug Metab. Dispos.* **1992**, *20*, 256−261.
(6) Porter, J. B.; Morgan, J.; Hoyes, K. P.; Burke, L. C.; Huehns, E. R.; Hider, R. C. Relative oral efficacy and acute toxicity of hydroxypyridin-4-one iron chelators in mice. *Blood* **1990**, *76*, 2389−2396.
(7) Porter, J. B.; Abeysinghe, R. D.; Hoyes, K. P.; Barra, C.; Huehns, E. R.; Brooks, P. N.; Blackwell, M. P.; Araneta, M.; Brittenham, G.; Singh, S.; Dobbin, P.; Hider, R. C. Contrasting interspecies efficacy and toxicology of 1,2-diethyl-3-hydroxypyridin-4-one, CP94, relates to differing metabolism of the iron chelating site. *Br. J. Haematol.* **1993**, *85*, 159−168.
(8) Bergeron, R.J.; Streiff, R.R.; Wiegand, J.; Luchetta, G.; Creary, E.A.; Peter, H.H. A comparison of the iron-clearing properties of 1,2-dimethyl-3-hydroxypyrid-4-one, 1,2-diethyl-3-hydroxypyrid-4-one, and Deferoxamine. *Blood* **1992**, *79*, 1882−1890.
(9) Porter, J. B.; Singh, S.; Hayes, K. P.; Epemolu, O.; Abeysinghe, R. D.; Hider, R. C. Lessons from preclinical and clinical studies with 1,2-diethyl-3-hydroxypyridin-4-one, CP94 and related compounds. *Adv. Expt. Med. Biol.* **1994**, *356*, 361−370.
(10) Singh, S.; Choudhury, R.; Epemolu, R. O.; Hider, R. C. Metabolism and pharmacokinetics of 1-(2′-hydroxyethyl)- and 1-(3'-hydroxypropyl)-2-ethyl-3-hydroxypyridin-4-ones in the rat. *Eur. J. Drug Metab. Pharmacokinet.* **1996**, *21*, 33−41.
(11) Liu, Z. D.; Lu, S. L.; Hider, R. C. *In vivo* iron mobilisation evaluation of hydroxypyridinones in ^{59}Fe-ferritin loaded rat model. *Biochem. Pharmacol.* **1999**, *57*, 559−566.
(12) Dobbin, P. S.; Hider, R. C.; Hall, A. D.; Taylor, P. D.; Sarpong, P.; Porter, J. B.; Xiao, G.; van der Helm, D. Synthesis, physicochemical properties, and biological evaluation of N-substituted 2-alkyl-3-hydroxy-4(1*H*)-pyridinones: Orally active iron chelators with clinical potential. *J. Med. Chem.* **1993**, *36*, 2448−2458.
(13) Rai, B. L.; Dekhordi, L. S.; Khodr, H.; Jin, Y.; Liu, Z.; Hider, R. C. Synthesis, Physicochemical properties and evaluation of N-substituted-2-alkyl-3-hydroxy-4(1H)-pyridinones. *J. Med. Chem.* **1998**, *41*, 3347−3359.
(14) Mitsunobu, O. The use of diethylazodicarboxylate and triphenylphosphine in synthesis and transformation of nature products. *Synthesis* **1981**, *1*, 1−28.
(15) Pippard, M. J.; Johnson, D. K.; Finch, C. A. A rapid assay for evaluation of iron chelating agents in rats. *Blood* **1981**, *58*, 685−692.
(16) Hider, R. C.; Khodr, H.; Liu, Z. D.; Tilbrook, G. Optimisation of pFe^{3+} values of iron(III) ligands with clinical potential. In *Metal Ions in Biology and Medicine Volume 5*; Collery, Ph., Brätter, P., Negretti de Brätter, V., Khassanova, L., Etienne, J.C., Eds.; John Libbey Eurotext: Paris, 1998; pp 51−55.
(17) Hider, R. C.; Epemolu, O.; Singh, S.; Porter, J. B. Iron chelator design. In *Progress in Iron Research;* Hershko, C., Konijn, A. M., Aisen, P. M., Eds.; Plenium Press: New York, 1994; Vol. 356, pp 343−349.
(18) Xu, J. D.; Kullgren, B.; Durbin, P. W.; Raymond, K. N. Specific sequestering agents for the actinides. 28: Synthesis and initial evaluation of multidentate 4-carbamoyl-3-hydroxy-1-methyl-2(*1H*)-pyridinone ligands for *in vivo* plutonium(IV) chelation. *J. Med. Chem.* **1995**, *38*, 2606−2614.
(19) Achmatowicz, Jr., O.; Bukowski, P.; Szechner, B.; Zwierzchowska, Z.; Zamojski, A. Synthesis of methyl 2,3-dideoxy-DL-alk-2-enopyranosides from furan compounds; A general approach to the total synthesis of monosaccharides. *Tetrahedron* **1971**, *27*, 1973−1996.
(20) Tate, B. E.; Miller, R. L. U.S.A. Patent 3 130 204, 1964.
(21) Ellis, B. L.; Duhme, A. K.; Hider, R. C.; Hossain, M. B.; Rizvi, S.; van der Helm, D. Synthesis, physicochemical properties, and biological evaluation of hydroxypyranones and hydroxypyridinones: Novel bidentate ligands for cell-labeling *J. Med. Chem.* **1996**, *39*, 3659−3670.
(22) Taylor, P. D.; Morrison, I. E. G.; Hider, R. C. Microcomputer application of nonlinear regression analysis to metal-ligand equilibria. *Talanta* **1988**, *35*, 507−512.
(23) Gran, G. Determination of the equivalence point in potentiometric titration. *Analyst* **1952**, *77*, 661−671.

JM991080O